JOURNAL OF MATERIALS SCIENCE 25 (1990) 1325–1330

Analysis of brittle fracture under the combined stresses of tension and compression

A. OKADA
Materials Research Laboratory, Central Engineering Laboratories, Nissan Motor Co., Ltd., 1, Natsushima-cho, Yokosuka, Kanagawa 237, Japan

Brittle fractures occurring under biaxial stress states were analysed based on the weakest link model using the mixed mode fracture criterion. Expressions for the mixed mode fracture criterion were chosen for application to the negative K_I region, corresponding to the compressive stress for the crack. Calculations for biaxial strength with randomly oriented constant-length cracks from the mixed mode fracture criterion were made in the region of $K_I > 0$ because an unstable fracture seems to occur in this region. The results indicated that the tensile stress component in the combined tension and compression stress state remains constant when the compressive component is smaller than the critical value, which is given by $[1 - (K_{IIc}/K_{Ic})^2]\sigma_t$ derived from the mixed mode fracture criterion, $(K_I/K_{Ic}) + (K_{II}/K_{IIc})^2 = 1$. Considering the statistical effects, however, calculation of the biaxial strength is modified to result in: (1) lowering the biaxial tensile strength, and in (2) a smooth transition from the constant tensile strength region to the decreasing strength region under the combined tension and compression stress. This suggests that the high K_{IIc}/K_{Ic} ratio results in the increase in the compressive strength relative to the tensile strength.

1. Introduction

The behaviour of the multiaxial fracture of brittle materials can be classified into two stress state groups: the tensile principal stress controlled fracture and the compressive principal stress controlled fracture. The former causes fractures owing to the rapid crack growth when one of the stress intensity factors for the pre-existed cracks reaches the critical value. The fracture strength in this case is provided by using the mixed mode fracture criterion. In the latter case, however, determining the theoretical fracture strength is complicated because the eventual fracture occurs after stable crack growth and the coalescing of the extended cracks [1–3]. Complication also arises owing to the technical problem of measuring the compressive strength, specifically, insufficient lubrication at the end points of the compression specimens results in a higher compressive strength estimation [4–5].

The multiaxial fracture comprising the compressive stress state will need further study relative to the phenomenon during fracture. This is because the simple weakest link model is difficult to apply when the major stress state is compressive. The application of the weakest link model is limited to the stress state where the normal stress for the crack is tensile.

The objective of the present study was thus to explore the effects of the practical mixed mode fracture criterion on the multiaxial strength under compression and tension.

2. Calculation of multiaxial strength

Griffith's equation [6] is known to account for the multiaxial fracture of brittle materials under the tensile and compressive stress states. He assumed that the fracture occurs when the tensile stress around the ellipsoidal hole reaches the critical value. When the curvature of the hole is infinitely sharp, the biaxial stresses of σ_1 and σ_2 are given by [6]

$$(\sigma_1 - \sigma_2)^2 + 8\sigma_t(\sigma_1 + \sigma_2) = 0 \quad \text{for } \sigma_2/\sigma_1 < -3 \tag{1a}$$

and

$$\sigma_1 = \sigma_t \quad \text{for } -3 < \sigma_2/\sigma_1 < 1 \tag{1b}$$

where σ_t is a tensile strength.

Hoek and Bieniawski [2] indicated that Griffith's equation can be represented using Mohr's envelope as

$$\tau^2 = 4\sigma_t(\sigma_t - \sigma) \tag{2}$$

where τ and σ are the shear stress and the normal stress at the fracture surface, respectively. Representation of the biaxial strength using Mohr's envelope was also made by Sato [7] who proposed a new equation given by

$$\tau^b = m_0\sigma_t^{b-1}(\sigma_t - \sigma) \tag{3}$$

where b and m_0 are material-dependent constants. This equation is reported to provide good agreement with the experimental results when the value, b, is in the range from 2 to 3 [7, 8]. Moreover, Equation 3 agrees with Equation 2 derived from Griffith's equation when $m_0 = 4$ and $b = 2$.

The fracture strength of the brittle materials can be explained by fracture mechanics. Provided the

0022–2461/90 $03.00 + .12

fracture occurs under the mixed mode of K_I and K_{II}, Equations 2 and 3 are rewritten by

$$K_I/K_{Ic} + (K_{II}/K_{IIc})^k = 1 \quad (4)$$

where $k = 2$ and $K_{IIc} = 2K_{Ic}$ for Griffith's equation, and $K_{IIc} = m_0^{1/k} K_{Ic}$ with $k = b$ for Sato's equation.

Although this mixed mode fracture criterion is different from the conventional criterion such as the maximum energy release rate [9], the maximum normal stress [10], and the minimum strain energy density [11], Equation 4 can derive similar expressions to meet the conventional mixed mode fracture criterion by selecting the value of k and the K_{IIc}/K_{Ic} ratio. Furthermore, this equation is capable of producing expressions to meet the recent mixed mode fracture data [12–14]. This suggests that the apparent mode II fracture toughness, K_{IIc}, can be heightened by the frictional sliding of the fracture surface.

The mixed mode fracture criterion calculated from the crack-tip stress field and the displacement should not be applied to the region of negative K_I because the meaning as a parameter for describing the stress field and the displacement near the crack-tip becomes obscure in the region of negative K_I. However, provided the negative K_I corresponds to the compressive stress for the crack, namely $\sigma < 0$, the negative K_I has meaning as a parameter for describing the fracture criterion. The criterion in the region of the negative K_I seems to be affected by the friction effect at the crack faces. The compressive stress decreases the effective K_{II} value through the frictional force in the crack faces. This is because the crack-tip field and the displacement are fundamentally determined by the K_{II} mode stress intensity factor. The effective shear stress at the crack faces, τ^*, is reduced by the friction [3]:

$$\tau^* = \tau + \mu\sigma \quad (5)$$

where μ is a friction coefficient and the normal stress, σ, is negative during compression. Accordingly, the effective mode II stress intensity factor, K_{II}^*, derived from τ^* is given by

$$K_{II}^* = K_{II} + \mu K_I \quad (6)$$

Provided the brittle fracture occurs when $K_{II}^* \geqq K_{IIc}$ in the region of $K_I < 0$, the fracture criterion becomes

$$K_{II} + \mu K_I = K_{IIc} \quad (7)$$

Note that Equation 4 in the region of negative K_I is approximately consistent with Equation 7 provided the friction coefficient, μ, decreases slowly with the increasing compressive stress. The expression for Equation 4 in the region of $K_I < 0$, however, may be strictly different from Equation 7. Equation 4 could thus be used for the approximate estimation of biaxial strength instead of Equation 7 in the region of $K_I < 0$.

From the mixed mode fracture criterion comprising the negative K_I, the biaxial strength with randomly oriented constant-length cracks can be obtained as follows. Draw an inscribed circle to the mixed mode fracture criterion of K_I and K_{II} (as shown in Fig. 1), and let the K_I values K_{I1} and K_{I2} ($K_{I1} > K_{I2}$) represent the two points of the circle when $K_{II} = 0$. This circle is similar to Mohr's circle except for the use of the stress intensity factor rather than stress. This modified Mohr's circle is defined by

$$(K_I - K_{I1})(K_I - K_{I2}) + K_{II}^2 = 0 \quad (8)$$

The two principal stresses, σ_1 and σ_2 ($\sigma_1 > \sigma_2$), are expressed as

$$\sigma_1 = \sigma_t(K_{I1}/K_{Ic}) \quad (9a)$$

and

$$\sigma_2 = \sigma_t(K_{I2}/K_{Ic}) \quad (9b)$$

Since the tensile strength of σ_t is positive, the magnitude of the principal stresses are proportional to the K_{I1} and K_{I2} values. The inclined angle, θ, for the extending crack is also shown in Fig. 1. The contact points of the envelope with Mohr's circle are represented by the K_I and K_{II} values at the fracture.

When the stress intensity factor, K_I, is positive, these values produce an instantaneous fracture condition free of stable crack growth. However, the initiation of crack extension does not always correspond to the fracture strength in the negative K_I because the eventual fracture occurs after stable crack growth, and the crack coalesces.

Under the combined stresses of tension and compression, the fracture occurs at the constant tensile stress in the limited range of the applied compressive stress. This region is predicted to be $-3 < \sigma_2/\sigma_1 < 1$ from Griffith's equation. However, the experimental results show a material dependence: $-3.5 < \sigma_2/\sigma_1 < 1$

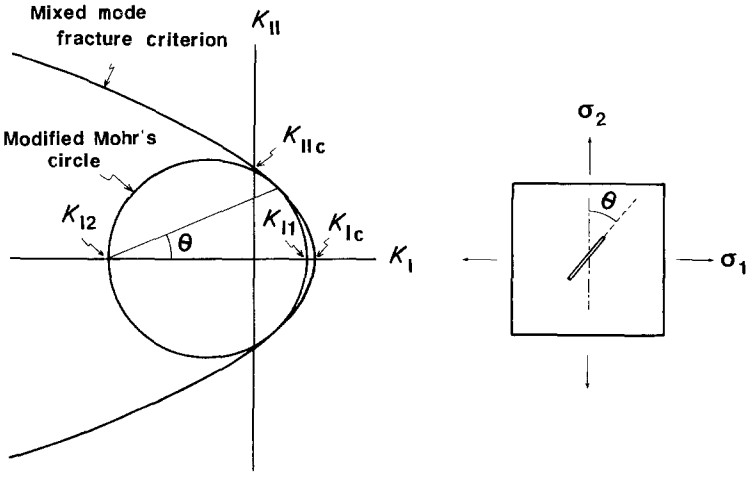

Figure 1 Schematic indication of the biaxial strength with randomly oriented constant-length cracks. The biaxial strength can be expressed by the stress intensity factors of K_{I1} and K_{I2} obtained from an inscribed circle to the mixed mode fracture criterion.

for plaster [7], $-1.4 < \sigma_2/\sigma_1 < 1$ for nodular iron [8], and $-1.2 < \sigma_2/\sigma_1 < 1$ for graphite [7]. This region is represented by $K_{I2}^*/K_{Ic} < \sigma_2/\sigma_1 < 1$, where K_{I2}^* is a K_{I2} value when the maximum Mohr's circle coincides internally with the mixed mode fracture criterion at the point of $K_I = K_{Ic}$. The biaxial strength can be calculated schematically from the arbitrary mixed mode fracture criterion.

Using the requirement of Mohr's circle coinciding internally with the mixed mode fracture criterion, the relationship between K_{II} and K_{I2} is obtained by combining Equations 4 and 8. When $k = 2$, it can be solved to obtain

$$K_{I2} = K_{II} - K_{IIc}^2/K_{Ic} - 2K_{IIc}(1 - K_{II}/K_{Ic})^{1/2} \quad (10)$$

When K_{II} equals to K_{Ic}, Equation 10 gives

$$K_{I2}/K_{Ic} = 1 - (K_{IIc}/K_{Ic})^2 \quad (11)$$

Accordingly, the region of the constant tensile stress component at the fracture under the combined tension and compression stress is given by

$$[1 - (K_{IIc}/K_{Ic})^2]\sigma_t < \sigma_2 < \sigma_t \quad (12)$$

This equation indicates that the constant tensile stress region appears when $K_{IIc} > K_{Ic}$, and that it spreads extensively with an increasing K_{IIc}/K_{Ic} ratio.

Figure 2 shows examples of calculated results of multiaxial fractures from the criterion derived by Equation 4 for $k = 2$ with K_{IIc}/K_{Ic} ratios of 1.0, 1.5, and 2.0. The K_I component at the fracture is obtained by combining Equations 4, 8 and 10, using the requirement of Mohr's circle coinciding internally with the mixed mode fracture criterion:

$$K_I = K_{I2} + K_{IIc}(1 - K_{I2}/K_{Ic})^{1/2} \quad (13)$$

The solid line in Fig. 2 shows the region of positive K_I, and the broken line shows the negative K_I region. The point at $K_I = 0$ appears in the area of decreasing tensile strength under the combined tension and compression stress. The biaxial fracture stresses at $K_I = 0$ are calculated from Equation 13 as

$$\sigma_1 = -(1/2)(K_{IIc}/K_{Ic})^2\{1 - [1 + 4(K_{Ic}/K_{IIc})^2]^{1/2}\}\sigma_t, \quad (14a)$$

and

$$\sigma_2 = -(1/2)(K_{IIc}/K_{Ic})^2\{1 + [1 + 4(K_{Ic}/K_{IIc})^2]^{1/2}\}\sigma_t, \quad (14b)$$

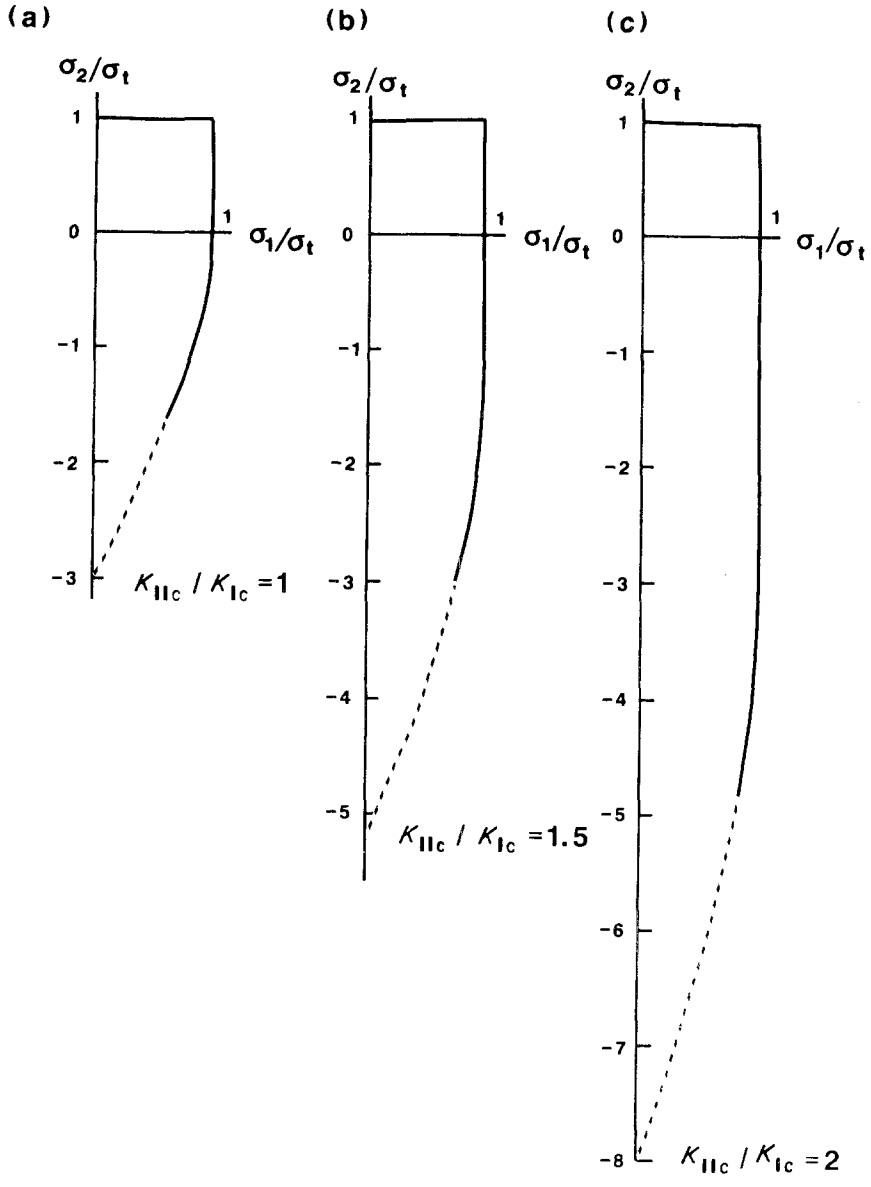

Figure 2 The biaxial strength with randomly oriented constant-length cracks calculated from the mixed mode fracture criterion $(K_I/K_{Ic}) + (K_{II}/K_{IIc})^2 = 1$; (a) $K_{IIc}/K_{Ic} = 1$, (b) $K_{IIc}/K_{Ic} = 1.5$, and (c) $K_{IIc}/K_{Ic} = 2$.

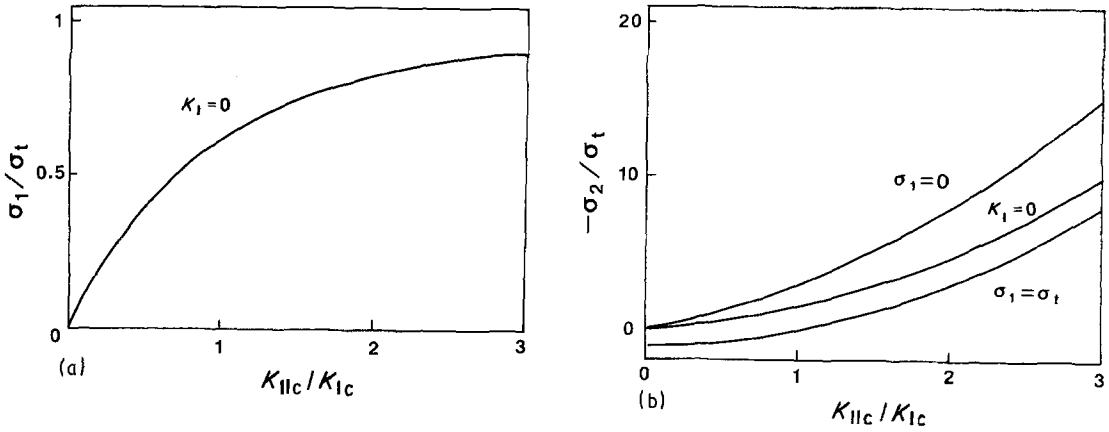

Figure 3 The principal stresses, σ_1 and σ_2, calculated as a function of K_{IIc}/K_{Ic}; (a) σ_1/σ_t at $K_I = 0$, (b) σ_2/σ_t at $\sigma_1 = 0$, σ_2/σ_t at $K_I = 0$, and σ_2/σ_t at $\sigma_1 = \sigma_t$.

Provided the stable crack growth does not occur prior to failure, the estimated compression strength, σ_c^*, can be given by letting $K_{II} = 0$ in Equation 10:

$$\sigma_c^* = -(K_{IIc}/K_{Ic})[(K_{IIc}/K_{Ic}) + 2]\sigma_t \quad (15)$$

This compressive strength may give a lower estimation because it neglects the stable crack growth prior to the final fracture.

Figure 3a shows the calculated results of the normalized principal stress, σ_1/σ_t, at $K_I = 0$, and Fig. 3b shows the values for $-\sigma_2/\sigma_t$ at $\sigma_1 = 0$, $K_I = 0$, and $\sigma_1 = \sigma_t$. These values increase with an increasing K_{IIc}/K_{Ic} ratio. When this K_{IIc}/K_{Ic} ratio increases from 0 to 3, the normalized stress, σ_1/σ_t, at $K_I = 0$ increases from 0 to 0.9, and the value $-\sigma_2/\sigma_t$ at $K_I = 0$ also increases from 0 to 10. Since the weakest link model can be applied to the region of $K_I > 0$, the appearance of the constant stress region of $\sigma_1 = \sigma_t$ will be explained in terms of the dependence on the K_{IIc}/K_{Ic} ratio. This is because the stress, σ_1, at $K_I = 0$ is lower than the tensile strength, σ_t, and the value of $-\sigma_2/\sigma_t$ at $\sigma_1 = \sigma_t$ is higher than that at $K_I = 0$. The value of σ_2/σ_t at $\sigma_1 = 0$, which corresponds to the compression strength when stable crack extension does not occur prior to fracture, also increases with the increasing K_{IIc}/K_{Ic} ratio.

Considering the statistical distribution of the cracks, the expression for biaxial strength should be modified. When brittle bodies containing N cracks are stressed, the fracture probabilities, P_f, are formulated as [15]

$$P_f = 1 - [1 - F(\sigma)]^N \quad (16)$$

and

$$F(\theta) = \int_0^{\pi/2} \frac{2}{\pi} \int_{a_c}^{\infty} f(a)\, da d\theta \quad (17)$$

Here, a_c, which depends on the mixed mode fracture criterion, is a minimum semi-crack length causing fracture as a function of the inclined angle, θ. The value, a_c, can be calculated from the criterion given by Equation 4, and when $k = 2$, it is expressed as (see Appendix)

$$a_c = [(-B + D^{1/2})/(2A)]^2 a_0 \quad (18)$$

with $A = \{[(\sigma_2/\sigma_1) - 1](K_{Ic}/K_{IIc})\}^2 \sin^2\theta(1 - \sin^2\theta)$, $B = 1 + [(\sigma_2/\sigma_1) - 1]\sin^2\theta$, $C = -1$, and $D = B^2 - 4AC$.

A function, $f(a)$, represents the probability density of the semi-crack length and is given by [15]

$$f(a) = [c^{n-1}/(n-2)!]a^{-n} \exp(-c/a) \quad (19)$$

where c is a scaling parameter and n is the rate at which the density tends toward zero. The scale factor, c, gives a maximum probability density when the semi-crack length is given by c/n. This expression was chosen to adopt Weibull statistics to the brittle fracture [16]. When the value of N is greater than the lowest limit given as a function of n, Weibull analysis yields a good approximation, and the values of m and n are related by $m = 2n - 2$ where the value, m, is the Weibull modulus with two-parameter function [15].

Figure 4 presents the calculated biaxial fracture considering fracture probability. In this calculation the parameters are chosen as $n = 4$, $c = 20\,\mu m$, $N = 100$, and the biaxial stresses for $P_f = 0.5$ are plotted. The outline of the biaxial fracture curve is similar to that in which the statistical effects are neglected. However, it is different in two points. One is a lowered biaxial tensile strength than the uniaxial tensile strength owing to the increase in the number of cracks responsible for the fracture. The other is the smooth transition from the constant tensile stress region to the decreasing tensile stress region under the combined tension and compression stresses.

3. Discussion

Some multiaxial fracture tests under compression and tension for brittle materials [7, 8, 17] have shown that a constant tensile stress is required to cause fracture when the compressive stress is lower than the critical stress. However, the constant tensile stress regions under compression and tension do not appear in porous ceramics [23] and ductile iron [8]. In these materials, the tensile stress component required for fracture gradually decreases with an increasing compressive stress. Since this inconsistency is derived from the dependence on the K_{IIc}/K_{Ic} ratio, it is attributed to the microscopic fracture behaviour of the material. The frictional force between the crack walls would affect the criterion not only in the region of negative K_I, but also in the region of $K_I > 0$ [12]. Considering

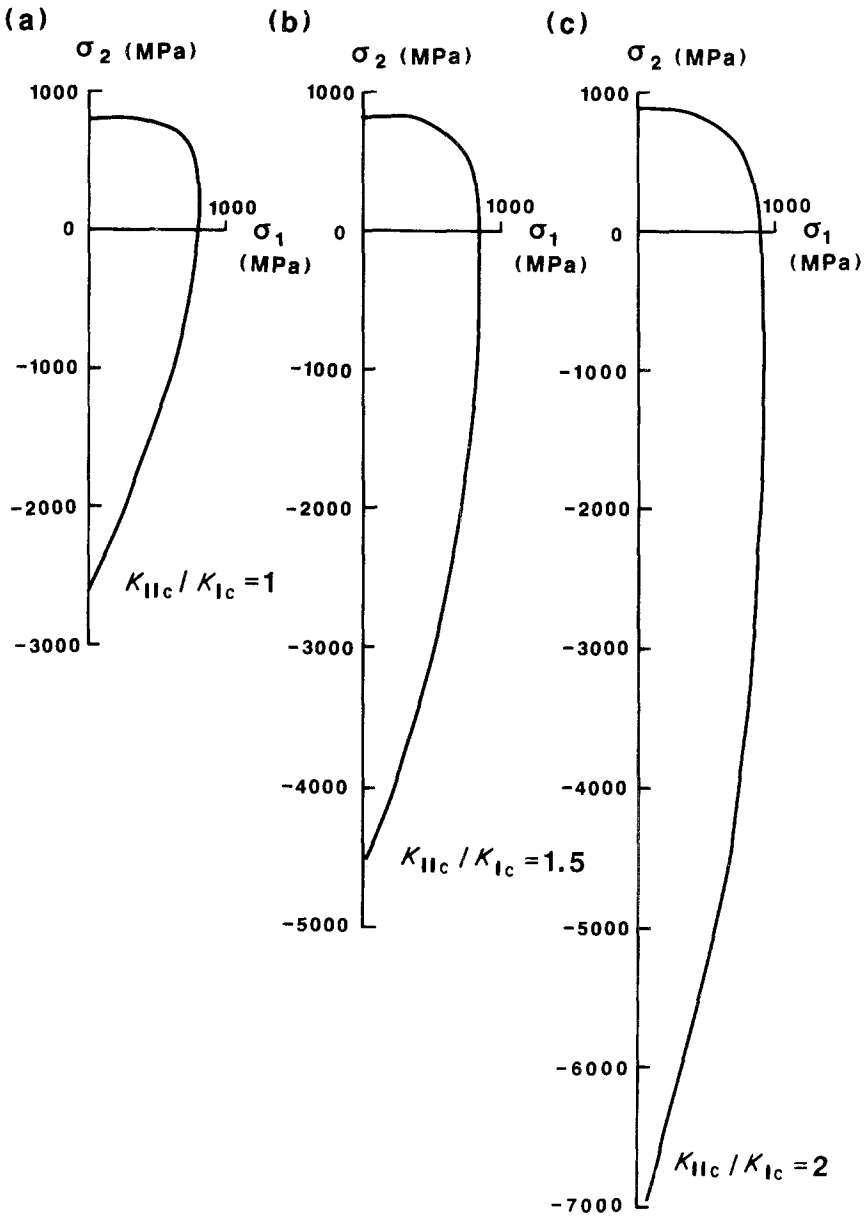

Figure 4 The biaxial strength considering fracture probabilities. The strength at $P_f = 0.5$ was calculated using Equations 16 to 19 with $n = 4$, $c = 20\,\mu m$, and $N = 100$.

that the frictional force resulting from the tortuosity of the crack extension leads to a steep slope in the R-curve in K_I mode fracture [18–20], the decrease in the K_I value results in an increase in the contact area in the crack walls through the decrease in the crack opening displacement. Consequently, the friction effects should still be more significant in the mixed mode fracture of K_I and K_{II}.

Provided the frictional force in the crack faces leads to a high K_{IIc}/K_{Ic} ratio, it should be strongly influenced by the microstructure of the materials and the crack configuration. There are three requirements for increasing the K_{IIc}/K_{Ic} ratio. One is to avoid separation of the cracks walls by minimizing the crack-tip blunting originated from the movement of dislocations at the highly stressed crack-tip field. Another is to provide hard contact in the crack walls by producing rough fracture surfaces. The other is not to reduce the frictional forces through a dropping of the particles from the contacting crack walls or by plastic deformation at the contacting points. From this viewpoint, the increased ratio of K_{IIc}/K_{Ic} or K_{IIIc}/K_{Ic} due to the friction effect is found in dense ceramics with sharp cracks.

Higher fracture toughness ratios than the prediction from the conventional theories neglecting friction effects are reported in alumina with $K_{IIIc}/K_{Ic} = 2.3$ [12], glass–ceramics with $K_{IIc}/K_{Ic} = 2.8$ [13], and silicon nitride with $K_{IIc}/K_{Ic} = 1.3$ [14]. However, when the distance between the crack walls is too wide to bring about mechanical interaction or the stress at the contacting points of the crack walls is easily released, the frictional effects are smaller. For instance, the measured ratio for low carbon steel is reported to be $K_{IIc}/K_{Ic} = 0.7$ [21]. This is within the range of the ratio predicted by the conventional theories because the plastic deformation and the thick slot introduced for measurement reduce the frictional force.

When the major stress is compressive in the combined stress state of compression and tension, it is extremely difficult to determine the close relationship between the K_{IIc}/K_{Ic} ratio and the fracture strength ratio of compression to tension, σ_c/σ_t. This is because the weakest link model is difficult to apply when the final fracture occurs after considerable crack extension. However, the first step in brittle fracture is crack extension from a pre-existing crack even under the compressive stress state. As a result, the weakest link model may provide the lowest estimation for the compression strength.

Although these effects should be incorporated, Equation 14 suggests that the compression strength, σ_c, relative to σ_t originates from the ratio of K_{IIc}/K_{Ic}. For instance, dense alumina with a 2.3% porosity, which is expected to have a high K_{IIc}/K_{Ic} ratio, has a high ratio of $\sigma_c/\sigma_t = -7$ [22]. Furthermore, materials expected to have a low K_{IIc}/K_{Ic} ratio have a low compression strength relative to the tensile strength: graphite with a 21% porosity has a ratio of $\sigma_c/\sigma_t = -2.3$ [22], and porous ceramic plate has a ratio of $\sigma_c/\sigma_t = -4.2$ [23].

It is obvious that considerable work remains to be done in the area related to the mixed mode fracture criterion and multiaxial fracture. Though this paper does not explain all the experimental results obtained by many authors, the frictional force between the crack walls is believed to play a substantial role in brittle fracture.

4. Conclusion

The multiaxial strength of a brittle solid was calculated from the mixed mode fracture criterion. The expression for the criterion chosen to exhibit capabilities for the various theories and the experiments is given by

$$K_I/K_{Ic} + (K_{II}/K_{IIc})^k = 1.$$

This expression includes the parameters of K_{Ic}, K_{IIc} and k. Calculation for the case of $k = 2$ indicates that:

1. The region for the positive K_I is obtained as

$$\sigma_1 > \sigma_t(K_{IIc}/K_{Ic})^2\{[(K_{Ic}/K_{IIc})^2 + 1/4]^{1/2} - 1/2\},$$

and

$$\sigma_2 > -\sigma_t(K_{IIc}/K_{Ic})^2\{[(K_{Ic}/K_{IIc})^2 + 1/4]^{1/2} + 1/2\};$$

2. the region for the constant tensile stress component at the fracture ($\sigma_1 = \sigma_t$) appears when $\sigma_2 > \sigma_t[1 - (K_{IIc}/K_{Ic})^2]$ even in the biaxial stress states of tension and compression.

In the region of negative K_I, it is difficult to predict the fracture strength because of the crack extension prior to the fracture. However, the estimated compressive strength from the weakest link model assumption is given by $\sigma_c^* = -(K_{IIc}/K_{Ic})[(K_{IIc}/K_{Ic}) + 2]\sigma_t$, which suggests that the ratio of the compressive strength to the tensile strength increases with the increasing K_{IIc}/K_{Ic} ratio. Assuming the friction effect between the crack walls occurs, dense ceramics are expected to have a high K_{IIc}/K_{Ic} ratio and a high compression strength.

Appendix

The value of a_c for the criterion of Equation 4 can be obtained as follows. The normal stress, σ_N, and the shear stress, τ, for the inclined crack, having an inclined angle of θ to the principal stress are given by

$$\sigma_N = \sigma_1 \cos^2\theta + \sigma_2 \sin^2\theta \quad \text{(A1a)}$$

and

$$\tau = -\tfrac{1}{2}(\sigma_1 - \sigma_2)\sin 2\theta \quad \text{(A1b)}$$

respectively. The stress intensity factors for K_I and K_{II} are represented by

$$K_I = Y\sigma_N a^{1/2} \quad \text{(A2a)}$$

and

$$K_{II} = Y\tau a^{1/2} \quad \text{(A2b)}$$

Substituting Equations A1 and A2 into Equation 4 with $k = 2$, we obtain

$$\{[(\sigma_2/\sigma_1) - 1]K_{Ic}/K_{IIc}\}^2(a/a_0)\sin^2\theta(1 - \sin^2\theta) + \{1 + [(\sigma_2/\sigma_1) - 1]\sin^2\theta\}(a/a_0)^{1/2} - 1 = 0 \quad \text{(A3)}$$

where $a_0 = (K_{Ic}/Y\sigma_1)^{1/2}$. Since Equation A3 is a quadratic equation for $(a/a_0)^{1/2}$, it can be solved to give

$$a_c = a_0[(-B + D^{1/2})/(2A)]^2, \quad \text{(A4)}$$

where $A = \{[(\sigma_2/\sigma_1) - 1]K_{Ic}/K_{IIc}\}^2\sin^2\theta(1 - \sin^2\theta)$, $B = 1 + [(\sigma_2/\sigma_1) - 1]\sin^2\theta$, $C = -1$, and $D = B^2 - 4AC$.

References

1. W. F. BRACE and E. G. BOMBOLAKEIS, *J. Geophysical Res.* **68** (1963) 3709.
2. E. HOEK and Z. T. BIENIAWSKI, *Int. J. Fracture Mechanics* **1** (1965) 137.
3. M. F. ASHBY and S. D. HALLEM, *Acta. Metall.* **34** (1986) 497.
4. P. PAUL, in "Fracture", Vol. 2, edited by H. Liebowitz. (Academic Press, New York, 1969) p. 313.
5. H. AWAJI, *Trans. Jpn Soc. Mech. Eng.* **A47** (1981) 880.
6. A. A. GRIFFITH, in Proceeding of the 1st International Congress on Applied Mechanics (Delft, 1924) p. 55.
7. Y. SATO, *Jpn J. Mech. Eng.* **39** (1973) 1096.
8. I. CORNET and R. C. GRASSI, *J. Basic Eng.* **83** (1961) 39.
9. M. A. HUSSAIN, S. L. PU and J. UNDERWOOD, *in ASTM STP* **560** (1974) p. 2.
10. F. EROGAN and G. C. SIH, *J. Basic Eng.* **85** (1963) 519.
11. G. C. SIH, *Int. J. Fracture* **10** (1974) 305.
12. S. SURESH and E. K. TSCHEGG, *J. Amer. Ceram. Soc.* **70** (1987) 726.
13. D. K. SHETTY, A. R. ROSENFIELD and W. H. DUCKWORTH, *ibid.* **69** (1986) 1437.
14. J. J. PETROVIC, in "Fracture Mechanics of Ceramics", Vol. 6, edited by A. G. Evans, R. C. Bradt, D. P. H. Hasselman and F. F. Lange (Plenum, New York, 1983) p. 63.
15. A. DE S. JAYATILAKA and K. TRUSTRUM, *J. Mater. Sci.* **12** (1977) 1426.
16. W. WEIBULL, *J. Appl. Mech.* **18** (1950) 293.
17. G. TAPPIN, R. W. DAVIDGE and J. R. McLAREN, in "Fracture Mechanics of Ceramics", Vol. 3, edited by R. C. Bradt, D. P. H. Hasselman and F. F. Lange (Plenum, New York, 1978) p. 435.
18. A. BORNHAUSER, K. KROMP and R. F. PABST, *J. Mater. Sci.* **20** (1985) 2586.
19. M. V. SWAIN, *J. Mater. Sci. Lett.* **5** (1986) 1313.
20. P. L. SWANSON, C. J. FAIRBANKS, B. R. LAWN, Y. W. MAI and B. J. HOCKEY, *J. Amer. Ceram. Soc.* **70** (1987) 279.
21. T. YOKOBORI, Y. ISHIZAKI and T. YOKOBORI, *Trans. Jpn Soc. Mech. Eng.* **A46** (1980) 590.
22. L. J. BROUTMAN, S. M. KRISHNAKUMAR and P. K. MALLICK, *J. Amer. Ceram. Soc.* **53** (1970) 649.
23. T. J. CHEN and W. J. KNAPP, *ibid.* **67** (1984) 648.

Received 30 November 1988
and accepted 16 May 1989